THE JOURNAL OF PHYSICAL CHEMISTRY Letters

LETTER

pubs.acs.org/JPCL

# What Drives the Redox Properties of Model Green Fluorescence Protein Chromophores?

Kyril M. Solntsev,*[,†] Debashree Ghosh,[‡] Adrian Amador,[†] Mira Josowicz,[†] and Anna I. Krylov*[,‡]

[†]Department of Chemistry, Georgia Institute of Technology, Atlanta, Georgia 30332-0400, United States

[‡]Department of Chemistry, University of Southern California, Los Angeles, California 90089-0482, United States

Supporting Information

**ABSTRACT:** We report the first experimental determination of the oxidation potentials $E_{ox}^{0}$ (relative to the standard hydrogen electrode, SHE) of model green fluorescent protein (GFP) chromophores. Para-, meta, and ortho-hydroxy (4-hydroxybenzylidene-2,3-dimethylimidazolinone, HBDI) and methoxy (MeOBDI) derivatives were studied. $E_{ox}^{0}$ of the three isomers in acetonitrile are −1.31, −1.52, and −1.39 V, respectively. Electronic structure calculations reproduce the observed differences between the isomers and reveal that $E_{ox}^{0}$ follows the ionization energies (IEs), that is, p-MeOBDI has the lowest IE (6.96 eV in the gas phase) due to resonance stabilization of its cation, whereas the resonance is detuned in m-MeOBDI, resulting in more-negative $E_{ox}^{0}$. The observed meta and ortho effects in $E_{ox}^{0}$ are similar to the trends in p$K_a$. The effect of increased solvent polarity on absolute $E_{ox}^{0}$ (and especially on para-meta-ortho differences) was found to be small. The redox properties of GFP chromophores are driven by their structure and can be correlated with IEs, which can be exploited in predicting the properties of other fluorescent protein chromophores.

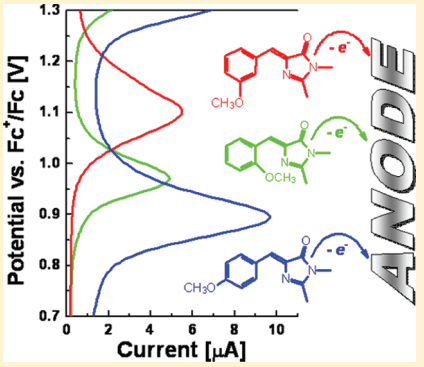


**SECTION:** Biophysical Chemistry

The unique properties of GFP exploited in novel bioimaging techniques have revolutionized many areas in the life sciences[1,2] and have motivated numerous experimental and theoretical studies.[3−7] To better understand the rich and complex photophysics of GFP, one can analyze its properties from bottom up, that is, from understanding the intrinsic properties of isolated FP chromophores to their behavior in the protein environment. Following this so-called reductionist approach, several studies have investigated model chromophores in the gas phase[8−10] and solutions.[11−15] Driven by mechanistic questions relevant to the GFP photocycle, these studies focused on optical properties of the chromophores, ground- and excited-state cis−trans isomerization, and acidity. A recent discovery that GFP can act as a light-induced donor of electrons[16] has brought the redox properties of FPs into the spotlight. In stark contrast with their optical properties, relatively little is known about the electron-detached (or ionized) states of FPs and, consequently, their redox properties. The gas-phase energetics of electron detachment of the anionic form of a model GFP chromophore, the deprotonated HBDI anion, has been characterized by electronic structure calculations,[17,18] and, subsequently, determined experimentally.[10] The effect of microsolvation and protein environment on detachment energy (DE) has been investigated computationally.[19] The protein matrix increases vertical DE (VDE) substantially (from 2.5 to 5.0 eV) via H-bonding and electrostatic interactions. $E_{ox}^{0}$ of the enhanced GFP mutant (EGFP) was estimated[19] to be −0.47 V. Experimentally, the production of solvated electrons and aromatic cation radicals has been observed for HBDI and its derivatives in solutions using femtosecond transient absorption.[11,14] Interestingly, the production of solvated electrons for the meta isomer in aqueous solution was much less efficient than that for p-HBDI.[11] It was suggested[14] that an ionization pathway may exist in the protein-bound GFP chromophore and that the transient absorption at 1.97 to 2.48 eV observed in the pump−probe experiment[20] might be due to solvated electrons rather than excited-state absorption. Redox potentials of the so-called redox-sensitive GFPs,[21] which change fluorescence in response to oxidation of surface cysteine groups, have been reported[22,23] (thus, the measured potentials correspond to the cysteine oxidation and not the chromophore). Another study reported reduction potential of the chromophore (resulting in the nonfluorescent form) in wtGFP.[24] Therefore, our study presents the first experimental characterization of the redox properties of model GFP chromophores in solution, which is a prerequisite for understanding the electron-donating properties of protein-bound chromophores. Knowledge of the redox potentials is important for developing generically encoded fluorescent redox probes,[21] understanding their phototoxicity[25] and using these chromophores in solar cell applications.[26] In addition to

**Received:** August 22, 2011
**Accepted:** September 26, 2011

  

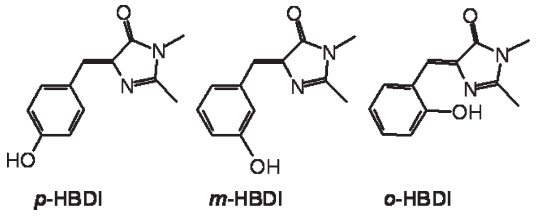


**Figure 1.** Para, meta, and ortho isomers of HBDI.

determining $E^0_{ox}$, we demonstrate that they are driven by the chromophores' structure and correlate with gas-phase IEs (i.e., HOMO energies).

We investigate the three model chromophores shown in Figure 1. As the electrochemistry of phenols is complicated by irreversible processes,[27,28] the experimental measurements were performed for the oxygen-methylated species, whereas the calculations characterized both methylated and nonmethylated systems. In the GFP chromophore, the phenolate oxygen is nonmethylated and is in the para position with respect to the methine bridge. The ortho and meta chromophores allow us to investigate the effect of structure on the redox properties. To eliminate the effect of specific H-bonding interactions with solvent, we performed the experimental measurements in an aprotic solvent, acetonitrile. (The solubility of the chromophores is also higher in acetonitrile than in water.) The calculations elucidate the effects of methylation and increased solvent polarity.

As discussed in numerous previous studies (e.g., refs 7, 29, and 30), an important feature of p-HBDI is resonance (mesomeric) interactions. In the deprotonated form, resonance leads to almost equal negative charge delocalization between the two CO moieties and profound bond-order scrambling. The meta form does not support the second resonance structure. This leads to structural changes and increased excitation energies. The protonation stabilizes the phenolate oxygen and partially detunes the resonance; however, one can still see its effects on equilibrium structures. For example, the difference between the two bridge CC bonds is smaller in p-HBDI (1.37 and 1.43 Å compared with 1.378 and 1.384 Å in the anion[17]) than in m-HBDI (1.35 and 1.46 Å). The latter is also nonplanar (see SM), which further destabilizes the conjugation. Because the resonance interactions are more pronounced in deprotonated HBDI, they lead to greater stabilization of the anionic form relative to the neutral, which results[11] in lower p$K_a$ of p-HBDI (8.5) relative to phenol (9.95) and m-HBDI (9.5).

The present study quantifies the effect of resonance interactions on the IEs and, consequently, the redox properties of the three chromophores. In terms of simple molecular orbital (MO) theory, IEs are related to the energies of the highest-occupied MO (HOMO). The oxidation potential is related to the change in the Gibbs free energy of the following process: HBDI $\rightarrow$ HBDI$^{+\bullet}$ + 1e via $E = -\Delta G/nF$, where $F$ is the Faraday's constant and $n$ is the number of transferred electrons. $\Delta G$, in turn, can be computed using the Hess cycle

$$\begin{aligned}\Delta G &= AIE + (\Delta G_{sol,\,HBDI^{+\cdot}} - \Delta G_{sol,\,HBDI}) \\ &= \mathrm{AIE} + \Delta\Delta G_{sol} \end{aligned} \quad (1)$$

where AIE is a gas-phase adiabatic IE and the $\Delta G_{sol,X}$ are solvation energies. The IEs were computed with DFT/cc-pVTZ using the range-separated dispersion-corrected $\omega$B97x-D functional.[31] The solvation free energies were calculated using the SM8 implicit solvation model.[32] All calculations were performed using *Q-CHEM*.[33] The HBDI isomers and their methyl ethers were synthesized and purified as previously described.[34−36] The experimental setup has been previously described.[37] Additional details of cyclic and differential pulse voltammetry measurements and the electronic structure calculations are provided in SM.

**Table 1. Calculated and Experimental $E^0_{ox}$ (V) versus the SHE**

| system | $E^0_{calcd}$ | $E^0_{exptl}$ | $E^0_{calcd}$-$E^0_{exprtl}$ |
|---|---|---|---|
| *para*-MeOBDI | −1.10 | −1.31 | 0.21 |
| *meta*-MeOBDI | −1.39 | −1.52 | 0.13 |
| *ortho*-MeOBDI | −1.24 | −1.39 | 0.15 |
| difference (p-m) | 0.29 | 0.21 | 0.08 |
| difference (o-m) | 0.15 | 0.13 | 0.02 |

**Table 2. Gas-Phase Vertical and Adiabatic Ionization Energies (electronvolts)**

| system | VIE | AIE | $E_{HOMO}$[a] | AIE with ZPE |
|---|---|---|---|---|
| *para*-HBDI | 7.37 | 7.06 | 7.46 | 7.06 |
| *meta*-HBDI | 7.66 | 7.39 | 7.76 | 7.37 |
| *ortho*-HBDI | 7.45 | 7.15 | 7.56 | 7.15 |
| difference (m-p) | 0.29 | 0.33 | 0.30 | 0.31 |
| difference (m-o) | 0.21 | 0.24 | 0.20 | 0.22 |
| *para*-MeOBDI | 7.28 | 6.96 | 7.40 | 6.96 |
| *meta*-MeOBDI | 7.55 | 7.29 | 7.67 | 7.27 |
| *ortho*-MeOBDI | 7.35 | 7.05 | 7.48 | 7.05 |
| difference (m-p) | 0.27 | 0.33 | 0.27 | 0.31 |
| difference (m-o) | 0.20 | 0.24 | 0.19 | 0.22 |

[a] Koopmans IE.

Table 1 summarizes the experimental and theoretical $E^0_{ox}$ values of the three MeOBDI isomers. It should be noted that it is only the relative rather than the absolute values that can be unambiguously determined experimentally because the experimental values of the working electrode are always referred to the potential of a reference electrode and depend on the unknown liquid junction potential between the reference electrode and the solution measured. However, the difference in $E^0_{ox}$ is not affected by these uncertainties. The experimental uncertainty in the relative redox potentials is <0.04 V for the compounds, as confirmed by repeated measurements, and is due to variations of the surface of the Pt electrode and is <0.005 V for the Fc/Fc+. The theoretical values, in turn, depend on the absolute potential of the SHE. In this work, we employ the most recent value[38] of 4.281 V and the variations in values obtained by other approaches (4.05 to 4.44 V, see refs 38 and 39) suggest an uncertainty in the absolute value of about ±0.2 V. Additional uncertainty in the computed $E^0_{ox}$ values is due to systematic errors of the implicit solvent models used to evaluate the contribution of solvation free energy ($\Delta\Delta G_{sol}$). On the basis of benchmark studies,[40,41] a conservative estimate of the error in computed $E^0_{ox}$ is 0.4 V; however, we expect that the relative differences between structurally similar compounds will be reproduced much more accurately by virtue of error cancellation. Indeed, as Table 1 demonstrates, the experimental and computed differences among p-, m-, and o-isomers are in remarkably good agreement. The discrepancies between theoretical and experimental absolute $E^0_{ox}$ are ∼0.2 V, which is less than the estimated error of the computed values.

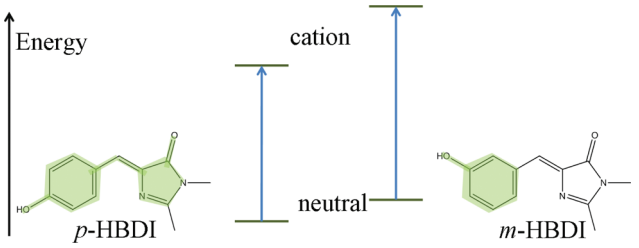


**Figure 2.** Relative energy levels of the neutral and ionized HBDI isomers. p-HBDI is stabilized relative to m-HBDI by resonance interactions that span the entire $\pi$-system. The resonance stabilization has larger effect on the energies of ionized species because it results in more extensive delocalization of the positive charge.

A linear fit of the experimental and computed values has $R^2$ = 0.99 (see SM). Overall, we consider the agreement between the theoretical and experimental values to be nearly perfect.

To analyze the observed trend in the $E^0_{ox}$ values, we begin by considering the AIEs of the isolated chromophores because according to eq 1, they provide the dominant contribution to $\Delta G$. The computed IEs summarized in Table 2 clearly demonstrate that the IEs increase in the para → ortho → meta series. This is somewhat counterintuitive because p-HBDI is more stable than m-HBDI owing to resonance stabilization, as reflected, for example, by the total electronic energies of the isomers. (p-HBDI is ~0.04 eV lower than m-HBDI; see SM.) However, resonance stabilization is more important in the cations, where it leads to more extensive hole delocalization. Therefore, the energy difference between the ionized isomers is larger than that in the neutral state (see Figure 2). Note that the respective Koopmans IEs (i.e., the HOMO energies) follow the computed IEs very well. Therefore, one can interpret the observed differences between the isomers in terms of the variation in the HOMO energy. The computed difference in the IEs is consistent with the experimentally observed reduced yield of solvated electrons for the meta-isomer relative to p-HBDI,[11] although one should also take into account the variation in the excited-state energy in view of the two-photon resonance-enhanced character of the ionization process in these experiments.[11,14]

The methylation results in a slight decrease in the IEs owing to the electron-donating properties of the $CH_3$ group; however, the overall effect is small (0.1 eV) and almost entirely cancels out when considering the relative differences between the isomers. The computed difference in $E^0_{ox}$ between the methylated and nonmethylated species is about −0.07 V.

The solvent effects are important for obtaining accurate absolute Gibbs energies and, consequently, redox potentials. Solvation energies in acetonitrile and water for the neutral and ionized species as well as resulting $\Delta\Delta G_{sol}$ are given in SM. The $\Delta\Delta G_{sol}$ terms reduce the IEs (and, respectively, $E^0$) by 1.4 to 1.6 eV; however, they are similar in all three isomers and, consequently, do not contribute toward the relative differences in the redox potentials, which are driven by AIEs. Overall, computed $E^0_{ox}$ in acetonitrile and water are remarkably similar (the differences <0.03 V). It should be noted, however, that implicit solvent models do not take into account possible effects of specific interactions (H-bonding). Therefore, such calculations only evaluate the changes in $E^0_{ox}$ due to solvent polarity. On the basis of previous experimental and computational studies,[42] the effect of solvent proticity might be as large as 0.2 V. The experiments in water are in progress now.

It is instructive to compare our oxidation potentials with previously reported values for phenols. $E^0_{ox}$ of 2,4,6-substituted phenols in acetonitrile[27] is −1.32 V. Phenol in water[43] has a more negative $E^0_{ox}$ of −1.52 V. These values are remarkably close to those of HBDIs, especially the meta-isomer, which is most similar to phenol owing to the absence of mesomeric interactions. The respective gas-phase IEs are also similar; that is, the computed gas-phase VIE of phenol is 8.48 eV. Phenolate has lower IE (2.25 eV, ref 44) and is easier to oxidize ($E^0_{ox}$ = −0.80 V in water[43] and −0.46 V in acetonitrile[45]). The anionic form of p-HBDI has similar gas-phase IE (2.39 eV, ref 18) and, therefore, is expected to have a similar redox potential. On the basis of the computed value of $E^0_{ox}$ in the protein (−0.27 V, ref 19), a less polar protein environment leads to less negative oxidation potential. Therefore, we expect that the neutral form of the protein-bound GFP chromophore will also have less negative $E^0_{ox}$ (by 0.2 to 0.3 V), relative to the measured values in acetonitrile.

In summary, the redox properties of GFP chromophores have been characterized for the first time. The structural differences among the p-, m-, and o-isomers affect $E^0_{ox}$ by 0.2 to 0.3 V via resonance stabilization of the respective cations. The analysis of computed free-energy components reveals that the trend in $E^0_{ox}$ is driven by the underlying IEs and can be correlated with the HOMO energy.

## ■ ASSOCIATED CONTENT

**Ⓢ Supporting Information.** Additional details of the electronic structure calculations and the experimental measurements, the geometries and relevant total energies of the neutral and cationic species, and the raw experimental data. This material is available free of charge via the Internet at http://pubs.acs.org.

## ■ ACKNOWLEDGMENT

This work was supported by NSF through the CRIF:CRF CHE-0625419 + 0624602 + 0625237 (iOpenShell Center), CHE-0951634 (A.I.K.), and CHE-0809179 (K.M.S.) grants.

## ■ REFERENCES

(1) Tsien, R. Y. The Green Fluorescent Protein. *Annu. Rev. Biochem.* **1998**, *67*, 509–544.

(2) Day, R. N.; Davidson, M. W. The Fluorescent Protein Pallete: Tools for Cellular Imaging. *Chem. Soc. Rev.* **2009**, *38*, 2887–2921.

(3) Zimmer, M. Green Fluorescent Protein (GFP): Applications, Structure, and Related Photophysical Behavior. *Chem. Rev.* **2002**, *102*, 759–781.

(4) Meech, S. R. Excited State Reactions in Fluorescent Proteins. *Chem. Soc. Rev.* **2009**, *38*, 2922–2934.

(5) Sample, V.; Newman, R. H.; Zhang, J. The Structure and Function of Fluorescent Proteins. *Chem. Soc. Rev.* **2009**, *38*, 2852–2864.

(6) van Thor, J. J. Photoreactions and Dynamics of the Green Fluorecent Protein. *Chem. Soc. Rev.* **2009**, *38*, 2935–2950.

(7) Bravaya, K. B.; Grigorenko, B. L.; Nemukhin, A. V.; Krylov, A. I. Quantum Chemistry Behind Bioimaging: Insights From Ab Initio Studies of Fluorescent Proteins and Their Chromophores. *Acc. Chem. Res.* **2011**, Article ASAP, DOI: http://dx.doi.org/10.1021/ar2001556.

(8) Nielsen, S. B.; Lapierre, A.; Andersen, J. U.; Pedersen, U. V.; Tomita, S.; Andersen, L. H. Absorption Spectrum of the Green Fluorescent Protein Chromophore Anion *In Vacuo*. *Phys. Rev. Lett.* **2001**, *87*, 228102.

(9) Rajput, J.; B., D.; Rahbek; Rocha-Rinza, L. H. A. T.; Christiansen, O.; Bravaya, K. B.; Erokhin, A. V.; Bochenkova, A. V.; Solntsev, K. M.; Dong, J.; Kowalik, J.; Tolbert, L. M.; Åxman Petersen, M.; Brøndsted Nielsen, M. Photoabsorption Studies of Neutral Green Fluorescent Protein Model Chromophores in Vacuo. *Phys. Chem. Chem. Phys.* **2009**, *11*, 9996–10002.

(10) Forbes, M. W.; Jockusch, R. A. Deactivation Pathways of an Isolated Green Fluorescent Protein Model Chromophore Studied by Electronic Action Spectroscopy. *J. Am. Chem. Soc.* **2009**, *131*, 17038–17039.

(11) Solntsev, K. M.; Poizat, O.; Dong, J.; Rehault, J.; Lou, Y.; Burda, C.; Tolbert, L. M. Meta and Para Effects in the Ultrafast Excited-state Dynamics of the Green Fluorescent Protein Chromophores. *J. Phys. Chem. B* **2008**, *112*, 2700–2711.

(12) Dong, J.; Abulwerdi, F.; Baldridge, A.; Kowalik, J.; Solntsev, K. M.; Tolbert, L. M. Isomerization in Fluorescent Protein Chromophores Involves Addition/Elimination. *J. Am. Chem. Soc.* **2008**, *130*, 14096–14098.

(13) Yang, J.-S.; Huang, G.-J.; Liu, Y.-H.; Peng, S.-M. Photoisomerization of the Green Fluorescence Protein Chromophore and the meta- and para-Amino Analogues. *Chem. Commun.* **2008**, 1344–1346.

(14) Vengris, M.; van Stokkum, I. H. M.; He, X.; Bell, A. F.; Tonge, P.; van Grondelle, R.; Larsen, D. S. Ultrafast Excited and Ground-state Dynamics of the Green Fluorescent Protein Chromophore in Solution. *J. Phys. Chem. A* **2004**, *108*, 4587–4598.

(15) Tolbert, L. M.; Baldridge, A.; Kowalik, J.; Solntsev, K. M. Collapse and Recovery of Green Fluorescent Protein Chromophore Emission Through Topological Effects. *Acc. Chem. Res.* **2011**, Article ASAP, DOI: http://dx.doi.org/10.1021/ar2000925.

(16) Bogdanov, A. M.; Mishin, A. S.; Yampolsky, I. V.; Belousov, V. V.; Chudakov, D. M.; Subach, F. V.; Verkhusha, V. V.; Lukyanov, S.; Lukyanov, K. A. Green Fluorescent Proteins are Light-induced Electron Donors. *Nat. Chem. Biol.* **2009**, *5*, 459–461.

(17) Epifanovsky, E.; Polyakov, I.; Grigorenko, B. L.; Nemukhin, A. V.; Krylov, A. I. Quantum Chemical Benchmark Studies of the Electronic Properties of the Green Fluorescent Protein Chromophore: I. Electronically Excited and Ionized States of the Anionic Chromophore in the Gas Phase. *J. Chem. Theory Comput.* **2009**, *5*, 1895–1906.

(18) Epifanovsky, E.; Polyakov, I.; Grigorenko, B. L.; Nemukhin, A. V.; Krylov, A. I. The Effect of Oxidation on the Electronic Structure of the Green Fluorescent Protein Chromophore. *J. Chem. Phys.* **2010**, *132*, 115104.

(19) Bravaya, K.; Khrenova, M. G.; Grigorenko, B. L.; Nemukhin, A. V.; Krylov, A. I. The Effect of Protein Environment on Electronically Excited and Ionized States of the Green Fluorescent Protein Chromophore. *J. Phys. Chem. B* **2011**, *8*, 8296–8303.

(20) Winkler, K.; Lindner, J.; Subramaniam, V.; Jovin, T. M. Ultrafast Dynamics in the Excited State of Green Fluorescent Protein (wt) Studied by Frequency-Resolved Femtosecond Pump-Probe Spectroscopy. *Phys. Chem. Chem. Phys.* **2002**, *4*, 1072–1081.

(21) Meyer, A.; Dick, T. Fluorescent Protein-Based Redox Probes. *Antioxid. Redox Signaling* **2010**, *13*, 621–650.

(22) Hanson, G. T.; Aggeler, R.; Oglesbee, D.; Cannon, M.; Capaldi, R. A.; Tsien, R. Y.; Remington, S. J. Investigating Mitochondrial Redox Potential with Redox-sensitive Green Fluorescent Protein Indicators. *J. Biol. Chem.* **2004**, *279*, 13044–13053.

(23) Dooley, C. T.; Dore, T. M.; Hanson, G. T.; Jakson, W. C.; Remington, S. G.; Tsien, R. Y. Imaging Dynamic Redox Changes in Mammalian Cells with Green Fluorescent Protein Indicators. *J. Biol. Chem.* **2004**, *279*, 2284–22293.

(24) Inouye, S.; Tsuji, F. I. Evidence for Redox Forms of the Aequorea Green Fluorescent Protein. *FEBS Lett.* **1994**, *351*, 211.

(25) Vegh, R. B.; Solntsev, K. M.; Kuimova, M. K.; Cho, S.; Liang, Y.; Loo, B. L. W.; Tolbert, L. M.; Bommarius, A. S. Reactive Oxygen Species in Photochemistry of the Red Fluorescent Protein "Killer Red". *Chem. Commun.* **2011**, *47*, 4887–4889.

(26) Chuang, W.-T.; Chen, B.-S.; Chen, K.-Y.; Hsieh, C.-C.; Chou, P.-T. Fluorescent Protein Red Kaede Chromophore; One-step, High-yield Synthesis and Potential Application for Solar Cells. *Chem. Commun.* **2009**, 6982–6984.

(27) Richards, J. A.; Whitson, P. E.; Evans, D. H. Electrochemical Oxidation of 2,4,6-Tri-*tert*-butylphenol. *J. Electroanal. Chem.* **1975**, *63*, 311.

(28) Evans, D. H.; Jimenez, P. J.; Kelly, M. J. Reversible Dimerization of Phenoxyl Radicals Formed by Anodic Ooxidation of Phenolates. A Quantitative Study by Cyclic Voltammetry. *J. Electroanal. Chem.* **1984**, *163*, 145.

(29) Olsen, S.; McKenzie, R. Bond Alternation, Polarizability, and Resonance Detuning in Methine Dyes. *J. Chem. Phys.* **2011**, *134*, 114520.

(30) Olsen, S. A Modified Resonance-Theoretic Framework for Structure-Property Relationships in a Halochromic Oxonol Dye. *J. Chem. Theory Comput.* **2011**, *6*, 1089–1103.

(31) Chai, J.; Head-Gordon, M. Long-range Corrected Hybrid Density Functionals with Damped Atom-atom Dispersion Interactions. *Phys. Chem. Chem. Phys.* **2008**, *10*, 6615–6620.

(32) Cramer, C. J.; Truhlar, D. G. A Universal Approach to Solvation Modeling. *Acc. Chem. Res.* **2008**, *41*, 760–768.

(33) Shao, Y.; Molnar, L. F.; Jung, Y.; Kussmann, J.; Ochsenfeld, C.; Brown, S.; Gilbert, A. T. B.; Slipchenko, L. V.; Levchenko, S. V.; O'Neil, D. P.; Distasio, R. A., Jr.; Lochan, R. C.; Wang, T.; Beran, G. J. O.; Besley, N. A.; Herbert, J. M.; Lin, C. Y.; Van Voorhis, T.; Chien, S. H.; Sodt, A.; Steele, R. P.; Rassolov, V. A.; Maslen, P.; Korambath, P. P.; Adamson, R. D.; Austin, B.; Baker, J.; Bird, E. F. C.; Daschel, H.; Doerksen, R. J.; Dreuw, A.; Dunietz, B. D.; Dutoi, A. D.; Furlani, T. R.; Gwaltney, S. R.; Heyden, A.; Hirata, S.; Hsu, C.-P.; Kedziora, G. S.; Khalliulin, R. Z.; Klunziger, P.; Lee, A. M.; Liang, W. Z.; Lotan, I.; Nair, N.; Peters, B.; Proynov, E. I.; Pieniazek, P. A.; Rhee, Y. M.; Ritchie, J.; Rosta, E.; Sherrill, C. D.; Simmonett, A. C.; Subotnik, J. E.; Woodcock, H. L., III; Zhang, W.; Bell, A. T.; Chakraborty, A. K.; Chipman, D. M.; Keil, F. J.; Warshel, A.; Herhe, W. J.; Schaefer, H. F., III; Kong, J.; Krylov, A. I.; Gill, P. M. W.; Head-Gordon, M. Advances in Methods and Algorithms in a Modern Quantum Chemistry Program Package. *Phys. Chem. Chem. Phys.* **2006**, *8*, 3172–3191.

(34) Dong, J.; Solntsev, K. M.; Tolbert, L. M. Solvatochromism of the Green Fluorescence Protein Chromophore and Its Derivatives. *J. Am. Chem. Soc.* **2006**, *128*, 12038–12039.

(35) Dong, J.; Solntsev, K. M.; Poizat, O.; Tolbert, L. M. The Meta-Green Fluorescent Protein Chromophore. *J. Am. Chem. Soc.* **2007**, *129*, 10084–10085.

(36) Chen, K.-Y.; Cheng, Y.-M.; Lai, C.-H.; Hsu, C.-C.; Ho, M.-L.; Lee, G.-H.; Chou, P.-T. Ortho Green Fluorescence Protein Synthetic Chromophore; Excited-State Intramolecular Proton Transfer via a Seven-Membered-Ring Hydrogen-Bonding System. *J. Am. Chem. Soc.* **2007**, *129*, 4534–4535.

(37) Li, Y.; Josowicz, M.; Tolbert, L. M. Diferrocenyl Molecular Wires. The Role of Heteroatom Linkers. *J. Am. Chem. Soc.* **2010**, *132*, 10374–10382.

(38) Isse, A. A.; Gennaro, A. Absolute Potential of the Standard Hydrogen Electrode and the Problem of Interconversion of Potentials in Different Solvents. *J. Phys. Chem. B* **2010**, *114*, 7894.

(39) Lewis, A.; Bumpus, J. A.; Truhlar, D. G.; Cramer, C. J. Molecular Modeling of Environmentally Important Processes: Reduction Potentials. *J. Chem. Educ.* **2004**, *81*, 596.

(40) Marenich, A. V.; Cramer, C. J.; Truhlar, D. G. Universal Solvation Model Based on Solute Electron Density and on a Continuum Model of the Solvent Defined by the Bulk Dielectric Constant and Atomic Surface Tensions. *J. Phys. Chem. B* **2009**, *113*, 6378–6396.

(41) Sviatenko, L.; Isayev, O.; Gorb, L.; Hill, F.; Lezczynski, J. Toward Robust Computational Electrochemical Predicting the Environmental Fate of Organic Pollutants. *J. Comput. Chem.* **2011**, *32*, 2195.

(42) Busch, M.; Knapp, E.-W. One-Electron Reduction Potential for Oxygen- and Sulfur-Centered Organic Radicals in Protic and Aprotic Solvents. *J. Am. Chem. Soc.* **2005**, *127*, 15730–15737.

(43) Costentin, C.; Louault, C.; Savéant, J.-M. The Electrochemical Approach to Concerted Proton-Electron Transfers in the Oxidation of Phenols in Water. *Proc. Natl. Acad. Sci. U.S.A.* **2009**, *106*, 18143–18148.

(44) Gunion, R. F.; Gilles, M. K.; Polak, M. L.; Lineberger, W. C. Ultraviolet Photoelectron Spectroscopy of the Phenide, Benzyl and Phenoxide Anions, with Ab Initio Calculations. *Int. J. Mass Spectrom. Ion Processes.* **1992**, *117*, 601–620.

(45) Hapiot, P.; Neta, P.; Pinson, J.; Rolando, C.; Schneider, S. Electrochemical and Radiolytic Mechanistic Studies on the Primary Step of Phenol Coupling Involved in Lignification. *New J. Chem.* **1993**, *17*, 21–224.